[SLAC-PUB-8789]
October 2000

Collagen Orientation and Crystallite Size in Human Dentin: A Small Angle X-ray Scattering Study*

J. H. Kinney, G.W. Marshall, S.J. Marshall
Department of Preventive and Restorative Dental Sciences, University of California, San Francisco, San Francisco, CA 94143-0758

J. A. Pople

Stanford Synchrotron Radiation Laboratory, Stanford Linear Accelerator Center, Stanford University, Stanford, CA 94309

Abstract

The mechanical properties of dentin are largely determined by the intertubular dentin matrix, which is a complex composite of type I collagen fibers and a carbonate-rich apatite mineral phase. We performed a small angle x-ray scattering (SAXS) study on fully mineralized human dentin to quantify this fiber/mineral composite architecture from the nanoscopic through continuum length scales. The SAXS results were consistent with nucleation and growth of the apatite phase within periodic gaps in the collagen fibers. These mineralized fibers were perpendicular to the dentinal tubules and parallel with the mineralization growth front. Within the plane of the mineralization front, the mineralized collagen fibers were isotropic near the pulp, but became mildly anisotropic in the mid-dentin. Analysis of the data also indicated that near the pulp the mineral crystallites were approximately needle-like, and progressed to a more plate-like shape near the dentino-enamel junction. The thickness of these crystallites, ~5 nm, did not vary significantly with position in the tooth. These results were considered within the context of dentinogenesis and maturation.

Keywords

dentin – collagen – mineralization - SAXS – dentinogenesis – orientation

Submitted to Calcified Tissues International

* Work supported by Department of Energy contract DE-AC03-76SF00515

INTRODUCTION

Dentin, the mineralized hard tissue that surrounds the pulp in teeth, is a composite of type I collagen interspersed with a carbonate-rich apatite mineral phase that gives it rigidity and strength [1]. Because dentin comprises the bulk of hard tissue in human teeth, its mechanical properties are of utmost importance in determining tooth strength. Changes in the mineral balance caused by caries, or disorganization of the collagen network caused by developmental or other disease-induced disorders, compromise the mechanical integrity of the tooth.

The most striking morphological feature of dentin is the tubule, the remnant home of the formative odontoblast process. It has long been thought that the tubule, with its hypermineralized peritubular cuff, influenced the mechanical properties of dentin [2]. The wide variance in the measured elastic constants was often attributed to variations in tubule density and orientation. However, now we have demonstrated that the intertubular dentin matrix, and not the dentinal tubules, dominates the elastic behavior [3]; the organization of the collagen-mineral complex is of paramount importance in this regard.

A complete understanding of the mechanical properties of dentin will require knowledge of the organization of the mineralized collagen fibrils at several length scales. At small length scales, the coupling of the mineral and organic phases controls the mechanical properties [4]. At larger length scales, the long-ranged alignment of the mineralized collagen fibrils affects the continuum elastic properties [5].

For the present study, we used the technique of small-angle x-ray scattering (SAXS) to determine the orientation of collagen in the intertubular dentin matrix. Analysis of the SAXS data also allowed us to describe the general shape of the mineral crystals and to estimate their size as a function of position in the circumpulpal dentin [6].

MATERIALS AND METHODS

Specimen Preparation

Three unerupted to partially erupted human third molars, with no visible or radiographic evidence of caries, were used in this study. Upon extraction, the teeth were gamma-irradiated for sterilization, [7] then stored whole in Hank's balanced salt solution and thymol. Immediately prior to study, a slow-speed diamond saw (Isomet; Buehler, Lake Bluff, IL) was used to cut thin (0.25 mm) occlusal wafers of circumpulpal dentin. The enamel, which girdled the specimen, was left intact as a fiducial reference for the location of the DEJ. The locations where the SAXS measurements were made are shown in Figure 1.

Small Angle X-ray Scattering

Small angle x-ray scattering was performed on beam line 1-4 at the Stanford Synchrotron Radiation Laboratory. A schematic of the experimental apparatus is shown in Figure 2. The synchrotron radiation from a bending magnet was focused in the vertical axis by applying a small curvature to a reflecting mirror in the optical train. The beam was made monochromatic at 0.149 nm by using the {111} reflection from a silicon single crystal. A small bend was applied to this crystal to provide the horizontal focus and increase the flux. Small lead apertures were used to collimate the beam size to 0.3 mm vertical by 0.35 mm horizontal at the specimen.

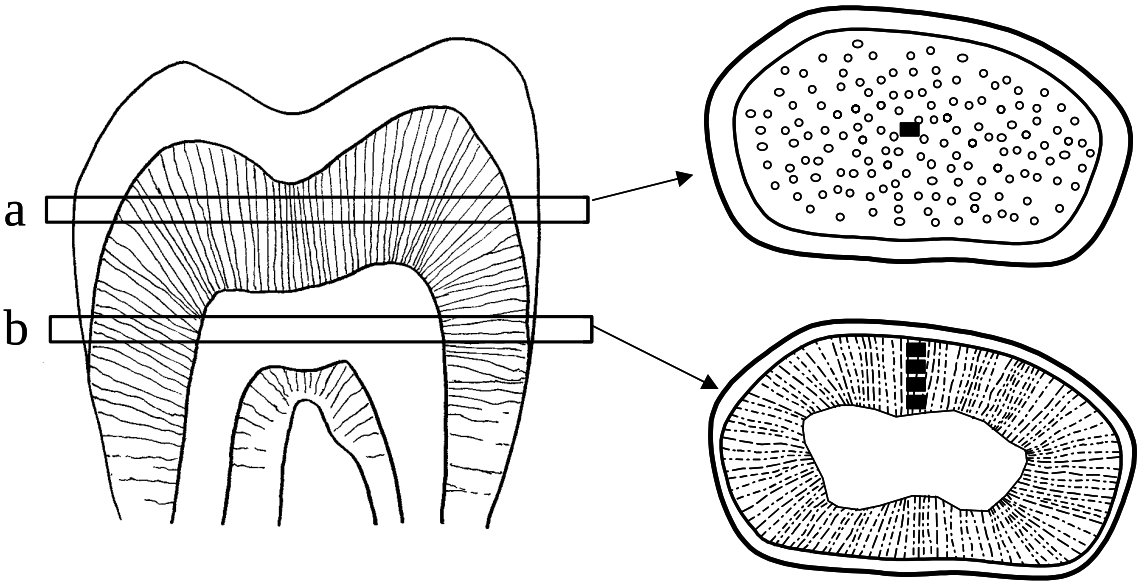

Figure 1: Coronal specimens were prepared from two regions of each tooth: a) immediately above the pulpal horn, and b) circumpulpal. The dark squares show locations where the SAXS data were obtained. Approximate orientations of the tubule lumens at each position have been hand drawn. For the circumpulpal dentin, the x-ray beam was scanned in 0.5 mm steps from the pulp outward in the bucal/lingual direction.

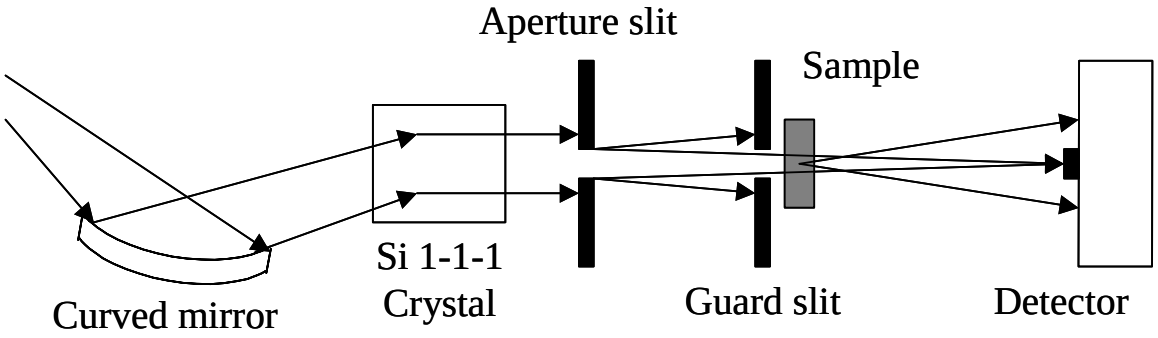

Figure 2: A schematic of the small angle x-ray scattering beamline 1-4 at Stanford Synchrotron Radiation Laboratory. X-rays from a bending magnet (SR) were focused in both the horizontal and vertical planes, and collimated with lead slits to create a point scattering geometry.

The x-ray beam was scanned across the specimens from the pulp to the DEJ in 0.5 mm steps. The SAXS data from each location was collected on two-dimensional imaging plate detectors (BAS-IIIs) and analyzed by the methods described below.

The two-dimensional scattering intensities, $I(x,y)$, were converted to polar coordinates, $I(q,\phi)$, where ϕ was the azimuthal scattering angle, and q was the wave vector given by:

$$q = \left(\frac{4\pi}{\lambda}\right)\sin\theta \qquad (1)$$

Here, λ was the incident x-ray wavelength, and 2θ was the scattering angle. Following the procedures described by Guinier [8], and applied to bone by Fratzl et al. [6, 9], the azimuthally averaged scattering intensity could be described as a function of q:

$$I(q) = I_o T^3 F(qT)(1 + G(q)) \qquad (2)$$

Here, the scattering form factor, $F(q,T)$, was a function of the shape of the crystallites, $G(q)$ was an interference function sensitive to correlations in the crystal positions, and T was a parameter related to the crystallite thickness.

Crystallite shape was inferred from the logarithmic dependence of q on the scattering intensity away from any scattering maxima. Though the word shape is frequently used when describing this logarithmic dependence, this term is somewhat a misnomer as there are no unique solutions to the inverse problem of defining shape directly from the scattering profiles. It is perhaps more appropriate to consider the form factor as providing a dimensionality, D: $F(q) \sim q^{-D}$. For D=1, the particle is roughly one-dimensional (i.e., length), and for D=2, the particle is two-dimensional (i.e., area). Based in part on electron microscopy [10] and the standard model of heterogeneous mineral nucleation in the collagen gaps [11, 12], it has been customary to refer to the one-dimensional scattering behavior as arising from needle-like shapes, and the two-dimensional scattering behavior as arising from plate-like crystals. We adopted this nomenclature for the present study.

The parameter T, which was associated with the crystallite thickness and had a unit of length, could be related to the total surface area, S, and the total volume, V, of the mineral crystals.

$$T = \frac{4V}{S} \qquad (3)$$

T was determined from Porod's observations of scattering at large q [8]:

$$I(q) \xrightarrow{\approx} \frac{P}{q^4}$$

$$T = \frac{4}{\pi P}\int q^2 I(q)\,dq \qquad (4)$$

The Porod constant, P, was determined by curve fitting the q^{-4} dependence of the scattering intensity at large q. The data were prepared as Kratky plots and the total scattering yield was calculated. Using the total scattering yield and the Porod constant P, the thickness parameter T was calculated directly from Equation 4. The thickness of the crystallites, τ, was estimated from the stereological relationship $\tau = T/2$.

The Guinier region of the SAXS data (small q limit) was analyzed by curve fitting the linear portion of the plot of ln I versus q^2 as q approached zero to obtain the slope, m. The radius of gyration, R_g, of the scattering crystals was estimated using the Guinier approximation:

$$R_g = \sqrt{3m} \qquad (5)$$

Orientation has been variously defined in terms of the areas under the profiles of the polar plots of the scattering intensity at single values of q. We have chosen, instead, to adopt a more physically robust measure of orientation, one that was developed to describe the molecular orientation within polymer melts and solutions [13]. Because the dimension of the illuminated specimen was large in relation to the size of the scattering units, the small angle scattering patterns provided a global average of an orientation distribution function, $O(\alpha)$, at each position in the specimen. To remove any contribution from fiber scattering off of the peritubular dentin, we investigated the azimuthal distributions of scattered intensity at the value of the scattering vector q corresponding with the third harmonic of the 67.6 nm reflection. In addition, care was taken to account for anisotropy in the background scattering that might have been caused by peritubular dentin. $O(\alpha)$, therefore, denoted the probability of finding a mineralized collagen fibril whose orientation could be described by the angle α to a prescribed axis, in this case the direction in the vertical scattering plane (bucal-lingual orientation of the tooth). The orientation distribution function, $O(\alpha)$, completely characterized the orientation of the fibrils; it was defined as a sum of orthogonal Legendre functions:

$$O(\alpha) = \sum_{n=0}^{\infty} (4n+1)\langle P_{2n}(\cos\alpha)\rangle P_{2n}(\cos\alpha) \qquad (7)$$

In equation 7, the globally averaged amplitude terms $< P_{2n}(\cos\alpha) >$ were used to describe the overall state of orientation. These coefficients were extracted directly from the small angle scattering patterns using the azimuthal distribution of the intensity function at a fixed value of q (here chosen to correspond with the third-order harmonic of the characteristic 67 nm diffraction peak). Because of the peak symmetry, only the even Legendre functions were needed to fit the data, and of these, only the first two even terms in Equation 7 were actually used. The second order term, $< P_2(\cos\alpha) >$, was evaluated from the data, and the ratio of its amplitude, $<P_2>_S$ to that of a model structure where all of the molecules were aligned in a single direction, $<P_2>_M$, was used to define the fraction of all collagen fibers aligned in a single orientation:

$$\langle P_2 \rangle = \frac{\langle P_2 \rangle_S}{\langle P_2 \rangle_M} \qquad (8)$$

Equation 8 was used to determine the fraction of the mineralized collagen fibrils that were preferentially aligned in the bucal/lingual orientation. For a perfectly random structure, this value would be zero; if all of the collagen fibrils were aligned in the direction of the model structure, this value would be 1.

RESULTS

A graph of the scattering intensity as a function of q for an x-ray beam incident parallel with mineralization front is shown in Figure 3. The profiles have been integrated for all scattering angles, ϕ, to minimize statistical fluctuations in the data. Marked in this figure

are the positions of the 67 nm reflection relating to the periodicity of the gap zones in the collagen fibrils (the actual measured spacing was ~67.6 nm corresponding to q = 0.0092 A^{-1}), and the third harmonic of this reflection at 22.6 nm (q = 0.028 A^{-1}). The precision of this measurement, which was controlled by the spatial resolution of the detector, was within 0.2 nm.

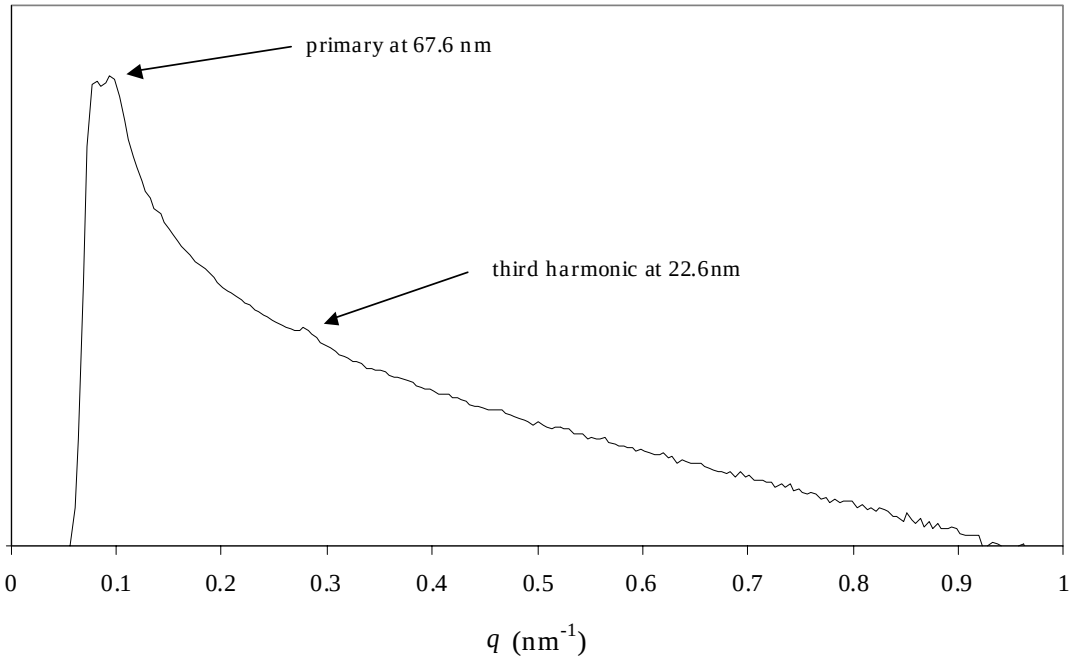

Figure 3: The azimuthally averaged SAXS pattern from a beam directed parallel to the plane of the mineralization front. The fundamental reflection at ~67.6 nm, and the third harmonic at ~22.6 nm were detected.

The scattering patterns from orientations perpendicular and parallel to the tubule axes are shown in Figure 4. Each trace was integrated over a 10° azimuthal range. The anisotropy of scattering was apparent by the presence of the harmonic when scattering perpendicular to the tubules and absence of the harmonic when scattering in the direction of the tubules.

The scattering intensity as a function of azimuthal angle at the third harmonic is shown in Figure 5 for a representative specimen. While there was no significant anisotropy in the background scattering, there was measurable azimuthal variation associated with the third harmonic. From this data, the orientation parameter was extracted. The orientation parameter for mineralized collagen fibrils lying in the plane of the mineralization front, $<P_2>$, is graphed as a function of position in Figure 6. Though there were relatively large differences between specimens, several trends were common in all teeth. First, the anisotropy was a minimum near the pulp. Second, the mineralized collage fibrils became progressively more anisotropic with distance from the pulp, reaching a maximum between 1-1.5 mm from the pulp. Finally, the magnitude of the peak anisotropy was less than 14%.

The decay exponent, or shape factor, for each tooth as a function of position is graphed in Figure 7. Nearest the pulp, the shape factor was most needle-like, ranging from 1.3 – 1.5; with distance from the pulp there was a continuous progression towards more plate-like shapes, ranging from 1.8 – 2.0 nearest the DEJ.

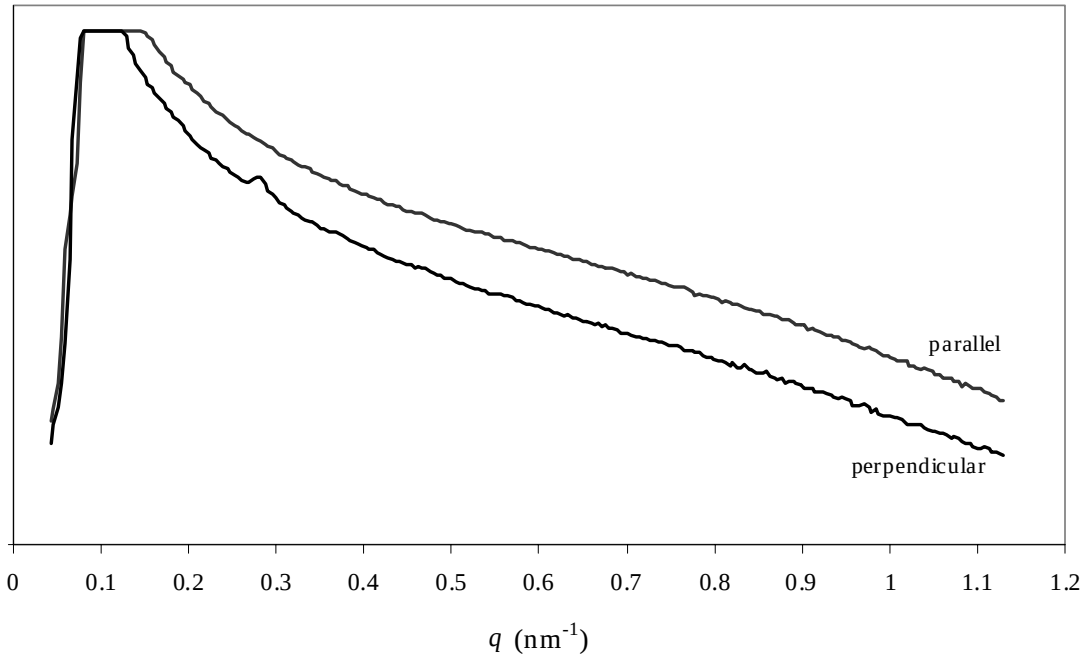

Figure 4: SAXS patterns from the same tooth directed parallel and perpendicular to the tubule axes. The harmonic reflection characteristic of the collagen fibril structure was only evident when the beam was perpendicular to the tubule axes, and in the plane of the mineralization front.

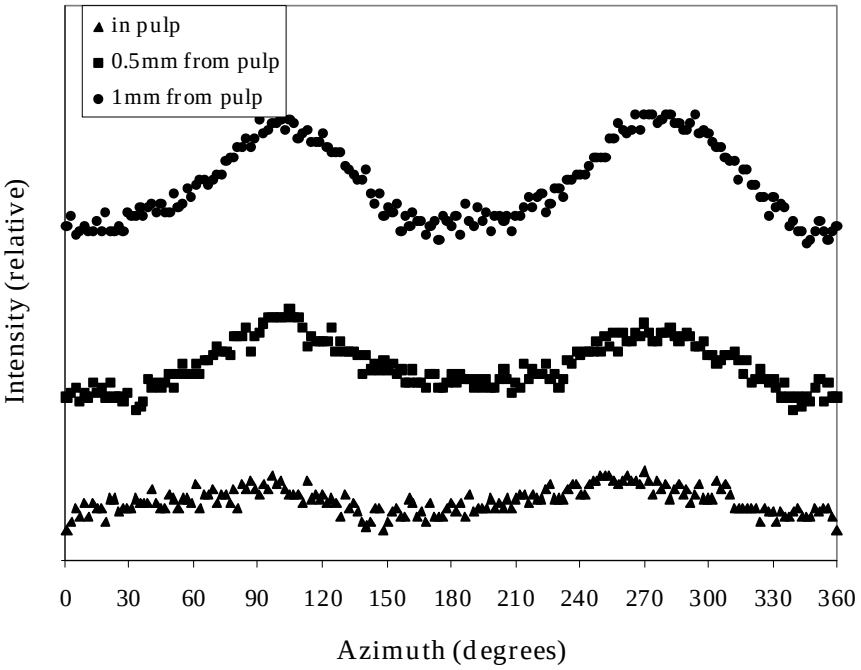

Figure 5: The scattering intensity as a function of azimuthal angle ϕ for a constant, small range of q (0.274-0.290 nm^{-1}) associated with the third harmonic of the 67.6 nm reflection. The symmetric peaks, whose magnitudes increased with distance from the pulp, were caused by a small anisotropy in one direction. The azimuthal angle $\phi = 0°$ was referenced to the bucal/lingual direction.

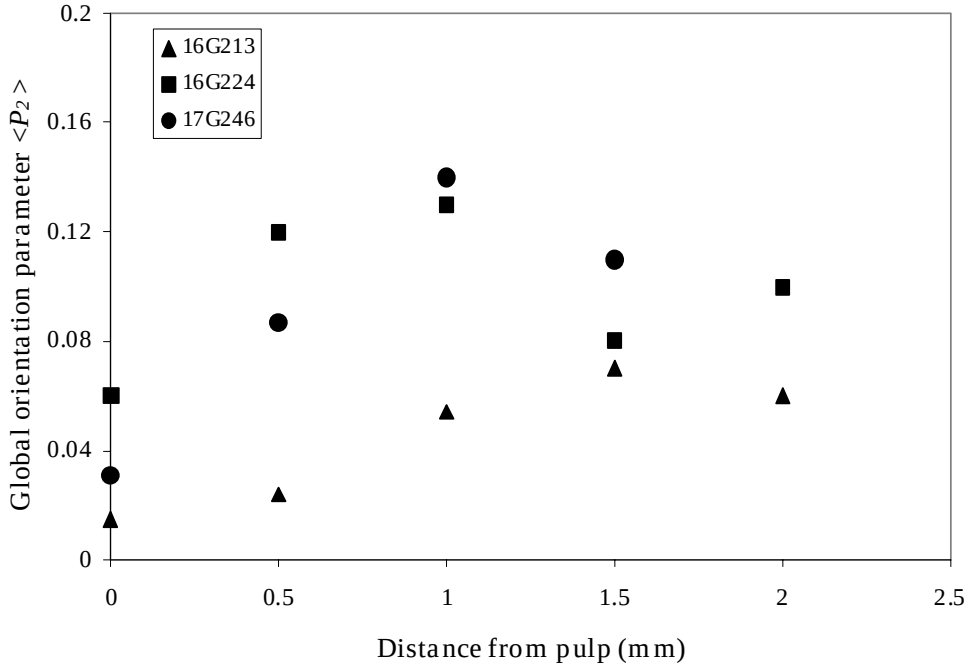

Figure 6: The global orientation parameter $<P_2>$ as a function of distance from the pulp. There was a gradual increase in anisotropy with distance, reaching a maximum between 1-1.5 mm from the pulp.

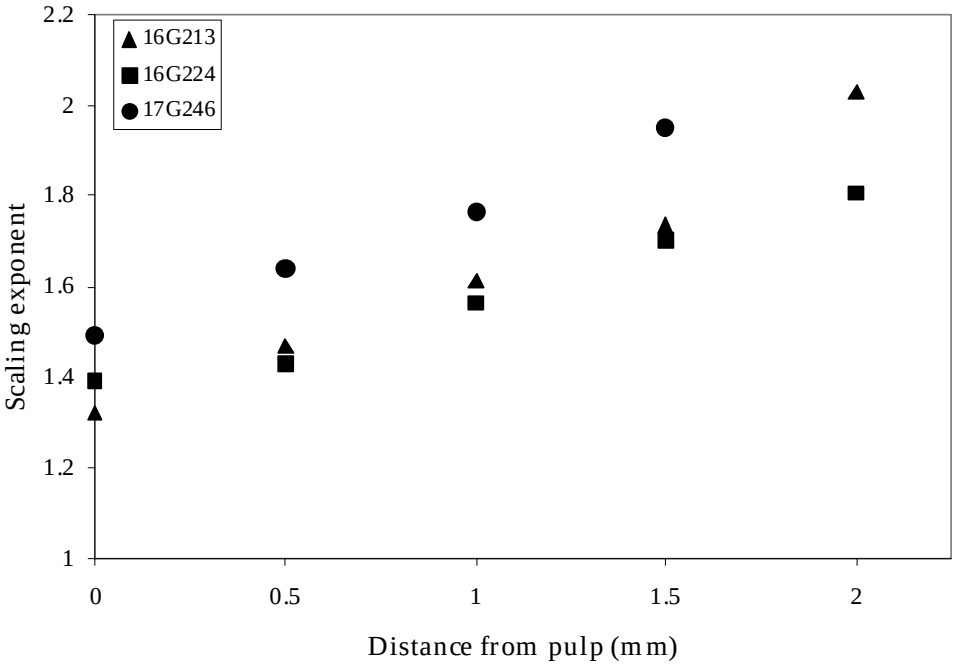

Figure 7: The decay exponent, or shape factor, as a function of distance from the pulp. The decay exponent was smaller near the pulp, and increased steadily with distance toward the DEJ. This was consistent with the shape gradually progressing from somewhat needle-like near the pulp to plate-like near the DEJ.

Crystallite thickness, τ, is graphed as a function of distance from the pulp in Figure 8. The mean thickness was roughly constant across the tooth, having a value of 5.0 nm (s.d. = 0.2 nm). The radius of gyration, R_g, was approximately 50 nm. The errors in the extremely low angle data, caused by both a shortened Guinier region and difficulty in making measurements at low-q, prevented a detailed analysis of the R_g as a function of position. It was noted, however, that linear behavior of ln$I$ vs. q^2 at low q (Guinier behavior) was only seen in the outermost dentin (nearest the DEJ).

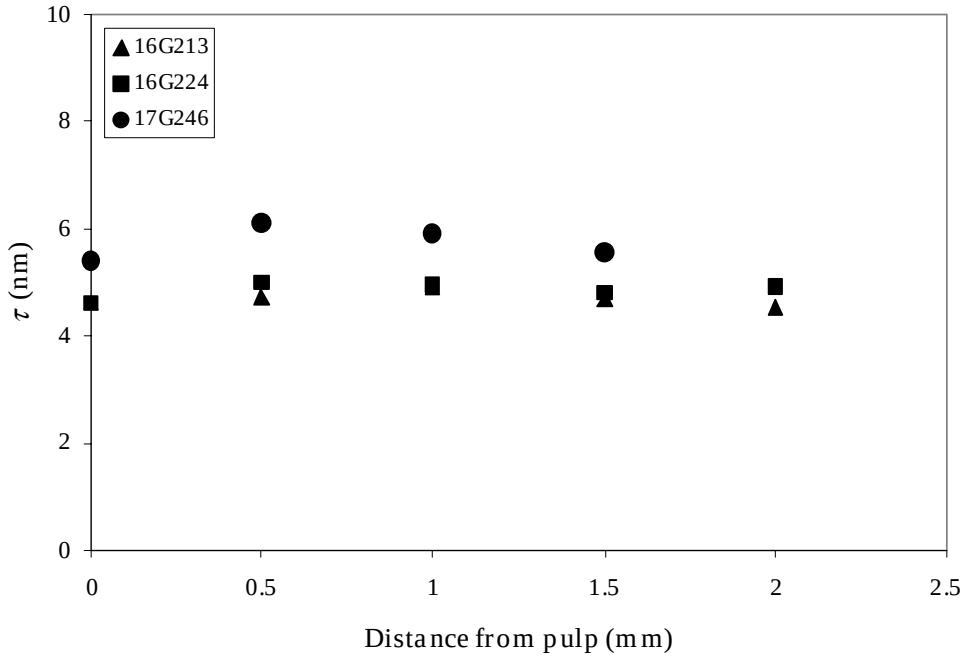

Figure 8: The mean thickness τ of the mineral crystallites as a function of distance from the pulp. There was no significant difference in thickness with position, in spite of the progressive change in shape of the crystallites.

DISCUSSION

To fully understand the mechanical properties of dentin, it is first necessary to know how the mineralized collagen fibrils are organized. It is generally believed that collagen fibrils form a felt work structure laid down perpendicular to the tubules and in the plane of the advancing mineralization front [14]. Exceptions to this organization have been reported; scanning electron microscopy of freeze-fractured specimens has occasionally shown collagen fibers having their long axes parallel with the tubule axes, although these fibers have largely been confined on the tubule walls adjacent to the odontoblast process [15, 16].

From prior studies in bone, a hallmark of the small angle scattering spectra is peaks in scattering intensity associated with an approximately 67-nm periodic spacing of gaps in the collagen fibrils [9]. According to the standard model of type I collagen mineralization, these gaps are primary sites for apatite crystal nucleation and growth [12]. By restricting our focus to the x-ray scattering associated with the allowed harmonics of this periodic spacing, we were reasonably assured of measuring the orientation of only the mineralized collagen fibrils.

It was significant that diffraction peaks were observed only when the incident beam was perpendicular to the tubules. When the incident x-ray beam was directed along the tubule axis, the diffraction peaks could not be detected. This was consistent with the majority of the mineralized collagen fibrils lying perpendicular to the tubules and in the plane of the mineralizing front.

It was possible to quantify the orientation of the mineralized collagen from the angular distribution of the scattered radiation. Adjacent to the pulp and within the plane of the mineralization front, the collagen fibrils were oriented isotropically: all angles of orientation were equally probable. With increasing distance from the pulp, the fibril orientation became progressively more anisotropic, reaching a maximum anisotropy in the dentin 1-1.5 mm from the pulp. The cause of this anisotropy is not known; we hypothesize it may be due to the change in formation rate between outer and inner dentin [11], or to an ordering of the tubule lumens that might allow short-ranged fibril alignment along one direction. Nevertheless, the measured anisotropy was not large: approximately 14% in the most extreme case. It is unlikely that this small structural anisotropy would have a measurable influence on dentin's elastic properties; earlier studies using AFM indentation methods were unable to detect anisotropy in the elastic modulus between orientations parallel and perpendicular to the tubule axis [3].

The shapes of mineral crystals have been studied in a variety of tissues [6, 10, 17, 18]. In mature human bone, it has been observed that the crystallites have a plate-like shape [6]. Plate-like crystals have also been observed in mineralizing tendon. These plate-like symmetries are in contrast to the needle-like crystals seen in less mature bone, and in bone undergoing more rapid turnover than seen in humans. The salient observation, however, is that the crystallite shape in bone appears to be of one type or the other, but not both, as represented by integral power law scaling of the SAXS data from those tissues [6,9].

Unlike bone, the SAXS data for dentin displayed non-integral power law scaling in all specimens. The apatite crystallites were somewhat needle-like near the pulp ($D\sim1.4$). With distance outward towards the DEJ, there was a continuous transformation to a more plate-like structure, becoming almost perfectly plate-like ($D\sim2$) near the DEJ. We attribute this transformation, which has no apparent counterpart in bone, to a maturation process. We propose that the crystallites are heterogeneously nucleated in the collagen gaps. With time, many of these needles can grow and coalesce into the plate-like structures seen in electron microscopy in bone. In the absence of remodeling, the crystallites are more plate-like in the dentin nearest the DEJ, and more needle-like in the more recently formed dentin adjacent to the pulp. We further propose that the non-integral power law scaling in the inner and middle dentin was the result of a distribution of needle- and plate-like crystallites.

Crystallite thickness (~5.0 nm), as determined from the Porod (large-q) region of the scattering curve, was consistent with earlier determinations (~4.0 nm) of crystallite size in dentin by x-ray powder diffraction methods [19]. Determination of crystallite size from x-ray powder diffraction patterns is not straightforward; there is no good way of separating the possible effects of strain broadening from those of size broadening because of the severe overlapping of the higher order peaks in the diffraction data. SAXS, on the other hand, is not affected by residual strain; hence, the close agreement between our measured thickness values and those determined from crystal diffraction indicate that size broadening dominates the x-ray diffraction behavior in dentin.

There was little variation in crystallite thickness with position in the tooth, even though their shapes changed significantly. This would suggest that crystal growth is constrained in one axis. We propose that the thickness is limited by the width of the gap

zone in the collagen fibril; the shape appears to evolve only by lateral growth and coalescence of adjacent crystallites.

The existence of a Guinier relationship at low-q is an interesting finding that should not be ignored. In a survey of half a century of SAXS literature on mineralized tissues, we were unable to find reference to Guinier analysis in the low-q region of the scattering pattern. There are, perhaps, two reasons for this. First, it is very difficult to make measurements at low q without resorting to specialized small angle cameras [20]. Second, interpretation of the low-q data is complicated in systems for which the Guinier approximation is not valid; for example, in systems that are not dilute. In dense systems like dentin, interparticle interference can significantly shorten the Guinier region and decrease the slope of the Guinier plot. Because of this, the radius of gyration is frequently underestimated.

Irrespective of these uncertainties, the existence of linearity in the graphs of ln I versus (q^2) indicated that there were features on the order of 50 nm or greater in radius that were coherently scattering the x-rays. We propose that the Guinier scattering at this length scale was consistent with scattering from the diameter of the mineralized collagen fibril, which is believed to vary from 60-200 nm.

To predict how age or disease-related changes in mineralization might affect dentin competence, it is important to know how mineral is proportioned between intra- and extra-fibrillar sites. A strong coupling of the mineral with the collagen fibrils would give dentin different properties than it would have if the mineral were entirely associated with the extrafibrillar ground matter [21]. The small angle scattering data implies that a nontrivial fraction of the mineral is intrafibrillar because of its association with the 67-nm gaps in the collagen fibrils. However, the data does not quantify what amount, if any, of the mineral might be extrafibrillar. Even in bone, which has been studied in far greater detail than dentin, the proportioning of extrafibrillar and intrafibrillar mineral is not known. We have even poorer knowledge of dentin mineralization. Resolution of this issue will require further studies with different imaging modalities.

In summary, the results of a small angle x-ray scattering study of healthy dentin were consistent with the majority of mineralized collagen fibrils lying within the plane of the mineralization front, and perpendicular to the tubules. Within this plane, the fibrils were virtually isotropic near the pulp; they became slightly anisotropic with distance from the pulp. The thickness of the mineral crystallites did not vary significantly with position in the tooth, although their shapes evolved from somewhat needle-like to plate-like with increasing proximity to the dentin-enamel-junction. What affect, if any, this change in crystallite morphology might have on the mechanical or etching properties of dentin requires further study.

ACKNOWLEDGMENTS

The National Institutes of Health, NIDCR, supported this work through grant PO1 DE09859. We acknowledge the support of the Stanford Synchrotron Radiation Laboratory (SSRL), U.S. Department of Energy, supported by Department of Energy contract DE-AC03-76SF00515. We acknowledge the contributions of D.L. Haupt for specimen preparation and Grace Nomomura for maintaining the documented tooth collection from which these specimens were selected.

REFERENCES

1. Marshall GW, Jr., Marshall SJ, Kinney JH, Balooch M (1997) The dentin substrate: structure and properties related to bonding. Journal of Dentistry 25:441-458
2. Sano H, Ciucchi B, Matthews WG, Pashley DH (1994) Tensile properties of mineralized and demineralized human and bovine dentin. Journal of Dental Research 73:1205-1211
3. Kinney JH, Balooch M, Marshall GW, Marshall SJ (1999) A micromechanics model of the elastic properties of human dentine. Archives of Oral Biology 44:813-822
4. Landis WJ (1995) The strength of a calcified tissue depends in part on the molecular structure and organization of its constituent mineral crystals in their organic matrix. Bone 16:533-544
5. Weiner S, Traub W, Wagner HD (1999) Lamellar bone: structure-function relations. Journal of Structural Biology 126:241-255
6. Fratzl P, Groschner M, Vogl G, Plenk H, Jr., Eschberger J, Fratzl-Zelman N, Koller K, Klaushofer K (1992) Mineral crystals in calcified tissues: a comparative study by SAXS. Journal of Bone and Mineral Research 7:329-334
7. White JM, Goodis HE, Marshall SJ, Marshall GW (1994) Sterilization of teeth by gamma radiation. Journal of Dental Research 73:1560-1567
8. Guinier A, Fournet G (1955) Small-Angle Scattering of X-rays. John Wiley and Sons, New York
9. Fratzl P, Fratzl-Zelman N, Klaushofer K, Vogl G, Koller K (1991) Nucleation and growth of mineral crystals in bone studied by small-angle X-ray scattering. Calcified Tissue International 48:407-413
10. Landis WJ, Hodgens KJ, Arena J, Song MJ, McEwen BF (1996) Structural relations between collagen and mineral in bone as determined by high voltage electron microscopic tomography. Microscopy Research and Technique 33:192-202
11. ten Cate AR (1994) Oral Histology: Development, Structure, and Function. Mosby, St. Louis
12. Hodge AJ, Petruska JA (1963) Recent studies with the electron microscope on ordered aggregates of the tropocollagen molecule. In: Ramachandran GN (ed) Aspects of protein structure. Academic Press, London, pp 289-300
13. Lovell R, Mitchell GR (1981) Molecular orientation distribution derived from an arbitrary reflection. Acta Crystallography A37:135-137
14. Johnson NW, Poole DFG (1967) Orientation of collagen fibers in dentine. Nature 213:695-
15. Jones SJ, Boyde A (1984) Ultrastructure of dentin and dentinogenesis. In: Linde (ed) Dentin and dentinogenesis. CRC Press, Boca Raton, pp 81-134
16. Dai X-F, Ten Cate AR, Limeback H (1991) The extent and distribution of intratubular collagen fibrils in human dentine. Archives of Oral Biology 36:775-778
17. Herold RC (1972) Fine structure of tooth dentine in human dentinogenesis imperfecta. Archives of Oral Biology 17:1009-
18. Landis WJ (1996) Mineral characterization in calcifying tissues: atomic, molecular and macromolecular perspectives. Connective Tissue Research 34:239-246
19. LeGeros RZ (1991) Calcium Phosphates in Oral Biology and Medicine. Karger, Basel
20. Pahl R, Bonse U, Pekala RW, Kinney JH (1991) SAXS investigations on organic aerogels. Journal of Applied Crystallography 24:771-776
21. Pidaparti RM, Chandran A, Takano Y, Turner CH (1996) Bone mineral lies mainly outside collagen fibrils: predictions of a composite model for osteonal bone. Journal of Biomechanics 29:909-916